

## THE INTRINSIC EVOLUTION OF $\text{Ly}\alpha$ -EMITTING GALAXIES FROM $z \approx 3$ TO THE EPOCH OF REIONIZATION

T. Garel<sup>1</sup>

**Abstract.** The evolution of the  $\text{Ly}\alpha$ -emitting galaxy population at  $z \gtrsim 6$  has become a popular tool to probe the reionization of the intergalactic medium.  $\text{Ly}\alpha$  photons arising from high redshift galaxies and travelling towards the observer can indeed be scattered off the line of sight by hydrogen atoms in the intergalactic medium, such that a rapid change of the observed  $\text{Ly}\alpha$  properties of galaxies can in principle trace the evolution of the IGM neutral fraction. However, in addition to intergalactic attenuation, the observability of  $\text{Ly}\alpha$  galaxies may also be (at least partially) driven by the intrinsic evolution of their physical properties and their internal  $\text{Ly}\alpha$  escape fraction. Here, we use a semi-analytic model of galaxy formation which accounts for the complex travel of  $\text{Ly}\alpha$  photons through galactic winds but neglects the effect of IGM absorption to discuss how intrinsic evolution alone affects the properties  $\text{Ly}\alpha$ -emitting galaxies at high redshift.

Keywords: galaxies: formation – galaxies: evolution – galaxies: high-redshift – radiative transfer – methods: numerical.

### 1 Introduction

$\text{Ly}\alpha$ -emitting galaxies are commonly observed from the ground at  $z \gtrsim 2$ -3 up to  $z \approx 7$ , allowing us to get insight into the first stages of galaxy formation. Of prime interest is the process of reionization which began when the first sources lit up and started heating up the gas and ionizing the intergalactic medium. The exact epoch at which reionization occurred, the nature of the sources responsible for it, as well as its impact on the formation and evolution of galaxies in the early Universe are still questions open to debate. Observationally, Gunn-Peterson trough measurements in quasar spectra show that the Universe was almost fully ionized by  $z \gtrsim 6$ , while the analysis of anisotropies in the CMB suggest that reionization started prior to  $z \approx 10$  (Becker et al. 2015; Planck Collaboration et al. 2016). In between ( $z \approx 6 - 8$ ), most constraints on the (volumetric) neutral fraction of the IGM,  $x_{\text{HI}}(z)$ , have been inferred from  $\text{Ly}\alpha$  emitter (LAE) observations (e.g. Ouchi et al. 2010; Schenker et al. 2014).  $\text{Ly}\alpha$  photons being resonantly scattered by HI atoms, the observability of the  $\text{Ly}\alpha$  line from high redshift galaxies can be strongly affected by IGM attenuation as the redshift increases, in particular when entering the epoch of reionization ( $z \approx 6$ ). Three main diagnostics have been suggested to probe  $x_{\text{HI}}(z)$  using  $\text{Ly}\alpha$ -emitting galaxies based on the redshift evolution of (i) the  $\text{Ly}\alpha$  luminosity function, (ii) the fraction of strong line emitters found in dropout galaxy surveys (i.e. among galaxies selected via their UV continuum magnitudes), and (iii) the clustering of LAEs. The interpretation of these observations with reionization models (e.g. McQuinn et al. 2007) favor an IGM neutral fraction of the order of  $\approx 50\%$  at  $z \approx 6.5 - 7$ . In most cases, the apparent change of the  $\text{Ly}\alpha$  properties at  $z \gtrsim 6$  is solely attributed to an increase of the neutral fraction of the IGM.

Here, in particular, we will discuss how the *intrinsic* evolution of the physical properties and the internal escape fraction of  $\text{Ly}\alpha$  photons affect the observability of LAEs at high redshift. We make use of a semi-analytic model of galaxy formation combined with a grid of  $\text{Ly}\alpha$  radiation transfer models (Garel et al. 2015). The semi-analytic model presented in Garel et al. (2015) is based on an updated version of GALICS (Hatton et al. 2003; Garel et al. 2016). GALICS describes the formation and evolution of galaxies in the cosmological context using (i) a N-body simulation to follow the growth of the dark matter structures and (ii) semi-analytic prescriptions to model the baryonic physics within the dark matter haloes identified in the simulation. We follow Garel et al.

---

<sup>1</sup> Univ Lyon, Univ Lyon1, Ens de Lyon, CNRS, Centre de Recherche Astrophysique de Lyon UMR5574, F-69230, Saint-Genis-Laval, France

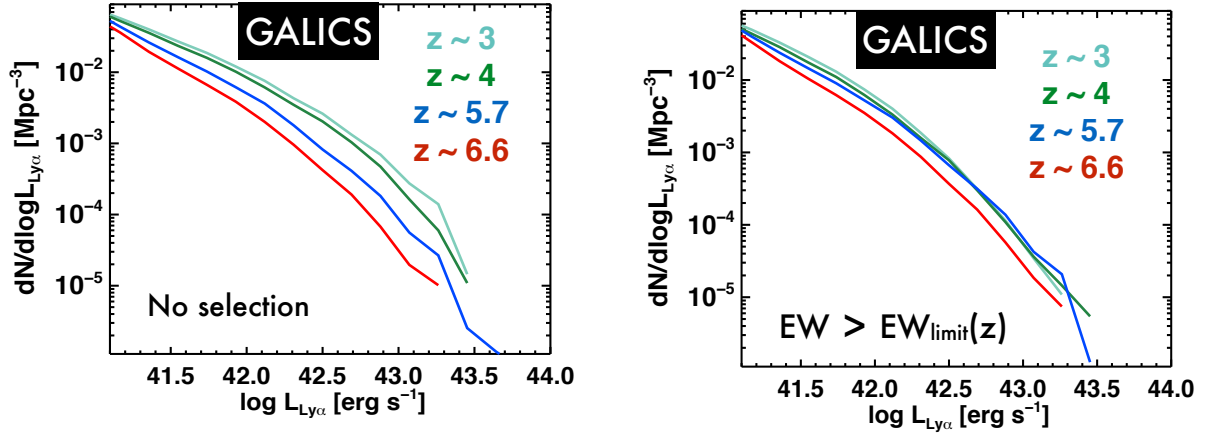


**Fig. 1. Left:**  $\text{Ly}\alpha$  LFs at  $z \approx 3, 4, 5.7$  and  $6.6$  as predicted by the Garel et al. (2015) model without LAE selection. **Right:** Same as the left panel but using an equivalent width limit to select LAEs.

(2012) to predict the  $\text{Ly}\alpha$  properties of each galaxy. The intrinsic  $\text{Ly}\alpha$  line is estimated from GALICS and described by a Gaussian profile centered on  $\lambda_\alpha$ . Observationally, there is growing evidence that the internal  $\text{Ly}\alpha$  escape fraction and the observed line profiles of galaxies both at low and high-redshift are primarily shaped by the presence of galactic outflows, presumably powered by supernovae (e.g. Steidel et al. 2010). We therefore compute the  $\text{Ly}\alpha$  radiation transfer using a simple wind model for GALICS galaxies (Garel et al. 2012) coupled with a grid of numerical simulations of  $\text{Ly}\alpha$  radiative transfer in expanding shells composed of HI gas and dust (Verhamme et al. 2008; Schaerer et al. 2011).

In the following sections, we compare our predictions to various existing  $\text{Ly}\alpha$  datasets and discuss at which extent *intrinsic* evolution alone can account for the observed evolution of the  $\text{Ly}\alpha$  luminosity function (LF), the fraction of strong emitters and LAE clustering at  $z \approx 6$ .

## 2 $\text{Ly}\alpha$ luminosity functions

In the left panel of Figure 1, we show the raw predictions from the Garel et al. (2015) model in which all LAEs at each redshift are used to construct the  $\text{Ly}\alpha$  LFs. In the model, the redshift evolution of the  $\text{Ly}\alpha$  LF is driven by the joint evolution of the star formation rate (SFR) and the  $\text{Ly}\alpha$  escape fraction of galaxies. On the one hand, the  $\text{Ly}\alpha$  LF is primarily driven by the evolution of the SFR function (since  $L_{\text{Ly}\alpha}^{\text{intr}} \propto \text{SFR}$ ) which increases in the model from  $z = 6$  to  $z = 3$  as a result of the growth of galaxies through gas accretion and mergers in a hierarchical Universe. On the other hand, we find that the average  $f_{\text{esc}}$  does not vary much with redshift, though there is a lot of dispersion from one galaxy to another depending on their own wind properties\*.

Based on SUBARU observations, Ouchi et al. (2008) report the non-evolution of the  $\text{Ly}\alpha$  LF between  $z = 3.1$  and  $z = 5.7$  and a sudden decrease from  $z = 5.7$  to  $z = 6.6$  (often associated to an increase of  $x_{\text{HI}}$ ), which is in contrast with our model predictions. In addition, Ouchi et al. (2010) find that the UV LF of LAEs seems to remain unchanged over this period. This suggests that, while the number density of LAEs does not vary, their observed  $\text{Ly}\alpha$  luminosity is reduced up to  $\approx 30\%$  (Ouchi et al. 2010; Hu et al. 2010; Kashikawa et al. 2011). To interpret the difference between our predictions and the SUBARU data, we now consider the impact of the LAE selection. The NB technique used by Ouchi et al. (2008, 2010) detects LAEs in wide-field surveys using various color criteria on the basis of an excess of flux in the NB. At first order, these criteria will select sources which have a rest-frame  $\text{Ly}\alpha$  equivalent width (EW) greater than a given limit,  $\text{EW}_{\text{limit}}$ . In the study of Ouchi et al. (2008, 2010), these  $\text{EW}_{\text{limit}}$  are higher at lower redshift, i.e. from  $\approx 60\text{\AA}$  at  $z \approx 3$  to  $15\text{\AA}$  at  $z \approx 6.6$ . In the right panel of Figure 1, we show the  $\text{Ly}\alpha$  LFs predicted by the model once we include this selection (in practice, we allow the  $\text{EW}_{\text{limit}}$  to vary by  $\approx 20\%$  around the value quoted by Ouchi et al. (2008, 2010)). We see that the

\*To test the additional effect of intervening gas on  $\text{Ly}\alpha$  fluxes, we used simple empirical prescriptions to model the  $\text{Ly}\alpha$  attenuation due to intergalactic absorbing systems. As discussed in Garel et al. (2015), we find an IGM transmission of nearly 100% in all cases because most  $\text{Ly}\alpha$  photons are redshifted away from resonance while escaping the galaxies through gas outflows in our model.

non-evolution of the LF from  $z = 3$  and  $z = 5.7$  can now be reproduced because the selection removes a larger fraction of LAEs at  $z \approx 3$  than at  $z \approx 6$ . Nevertheless, we note that spectroscopic surveys have also reported a constant Ly $\alpha$  LF evolution from  $z \approx 3$  and  $z \approx 6$  using fixed EW<sub>limit</sub> (Cassata et al. 2011), in agreement with the SUBARU data but in contradiction with our interpretation. However, the volume they probed was small so it is plausible that cosmic variance was affecting their results. In addition, we find that the  $z = 6.6$  Ly $\alpha$  LF is decreased by an amount of about 30% in terms of Ly $\alpha$  luminosity compared to the lower redshift LFs, in good agreement with the observed trend. Our results suggest that additional constraints using more homogeneous selection over large samples of LAEs seem necessary to fully exploit the Ly $\alpha$  LF evolution as a probe of  $x_{\text{HI}}$ .

### 3 LAE fraction

In the last years, many studies have intended to use the fraction of Ly $\alpha$  line emitter,  $X_{\text{LAE}}$ , in samples of dropout galaxies as a probe of  $x_{\text{HI}}(z)$ .  $X_{\text{LAE}}$  increases from  $z \approx 3$  to  $z \approx 6$  and seems to suddenly drop at  $z \approx 7$  (Stark et al. 2011; Schenker et al. 2014), possibly due to by a sharp increase of neutral IGM opacity at  $z \gtrsim 6$ <sup>†</sup>. In Figure 2, we show the redshift evolution of the fraction of strong (EW > 55Å; right panel) and weaker (EW > 25Å; left panel) Ly $\alpha$  emitters among UV-bright dropout galaxies.

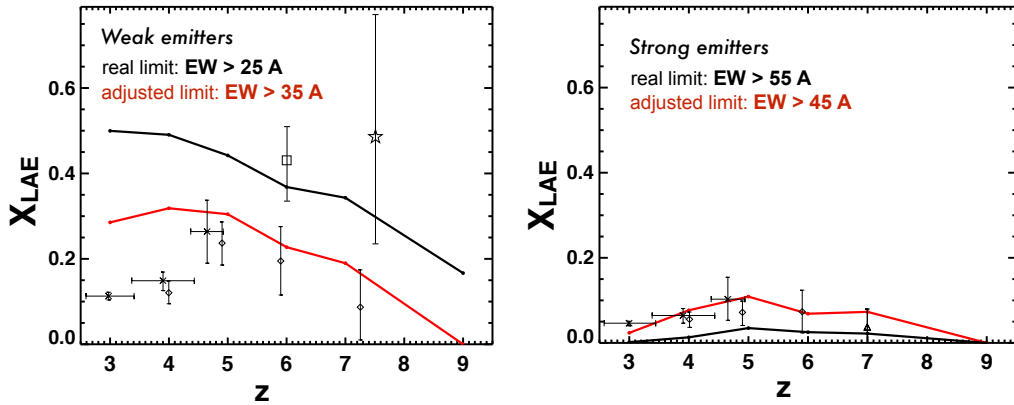


**Fig. 2.** Redshift evolution of the LAE fraction,  $X_{\text{LAE}}$ , in samples of bright dropout galaxies. The right and left panels show the redshift evolution of  $X_{\text{LAE}}$  for strong (EW > 55Å) and weaker (EW > 25Å) Ly $\alpha$  emitters respectively. The black curves represent the model predictions using the same EW limits as the ones used to derive the observational measurements (shown by the various data points; see the Figure 8 of Garel et al. (2015) for the references). The red curves show our predicted  $X_{\text{LAE}}$  if these limits are varied by 10Å.

In Figure 2, we show the comparison between observational data points and the predictions from our model (black curves) using the EW cuts that were used to compute  $X_{\text{LAE}}$  in the various dropout galaxies samples. We see that the model cannot reproduce the overall trend of  $X_{\text{LAE}}(z)$  neither for strong nor weak emitters. Then, we adjust the EW limits in order to get a better match with the observational data (red curves). We find that varying these cuts by only 10Å greatly improves the agreement and that the overall shape of the redshift evolution of  $X_{\text{LAE}}$  can be better recovered, i.e. a rise from  $z \approx 3$  to  $z \approx 5 - 6$  and then a drop at higher  $z$ . This result highlights that  $X_{\text{LAE}}(z)$  may strongly vary depending on the EW limits and that intrinsic evolution can partially govern the observed trends.

### 4 Clustering of LAEs

An alternative measurement to constrain the ionization state of the IGM can be provided by the 2-point angular correlation function (ACF) of LAEs. Indeed, as first shown by McQuinn et al. (2007), the visibility of LAEs when entering the EoR is favoured if these objects reside in large HII bubbles located at high density peaks, where haloes are strongly clustered. This translates into an apparent *boost* of the ACF, as shown by the results from the simulations of McQuinn et al. (2007) in the left panel of Figure 3: circles and crosses correspond to an IGM neutral fraction  $x_{\text{HI}}$  of 30% and 0% respectively. In contrast, the Garel et al. (2015) model does

<sup>†</sup>We note that some surveys have found that  $X_{\text{LAE}}$  keeps rising at  $z \gtrsim 6 - 7$ .

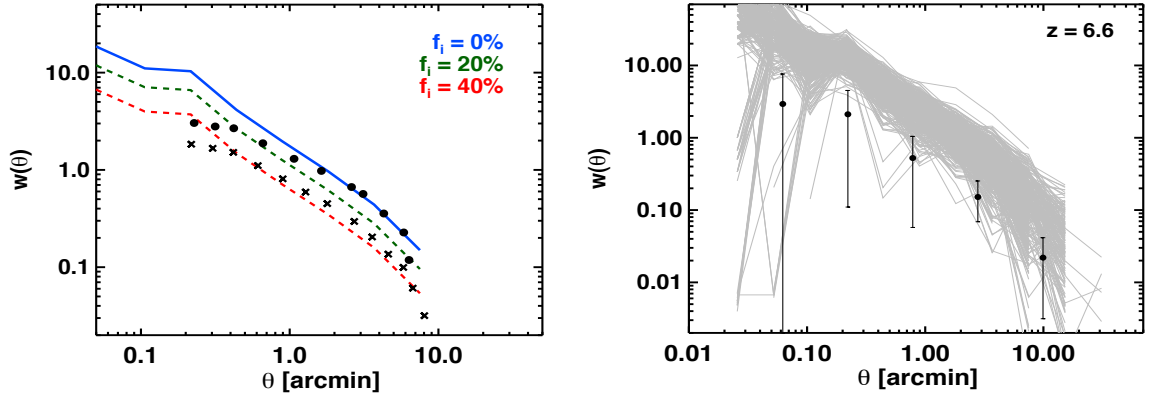


**Fig. 3.** 2-point angular correlation function of LAEs at  $z = 6.6$ . **Left:** ACF from the Garel et al. (2015) model for various fractions of interlopers among LAEs. Circles and crosses correspond to the simulations of McQuinn et al. (2007) for which the IGM neutral fraction  $x_{\text{HI}}$  is 30% and 0% respectively. **Right:** ACFs measured from 500 mock lightcones. Black dots are data points from the survey of Ouchi et al. (2010).

not follow the growth of HII bubbles during the EoR and, as discussed in Section 2, our IGM prescription for Ly $\alpha$  attenuation does not affect the Ly $\alpha$  luminosities. Therefore, here, we only investigate the ACF at  $z \gtrsim 6$  in terms of intrinsic evolution and discuss the expected effects of contamination and cosmic variance on the clustering of LAEs.

As discussed in McQuinn et al. (2007), the contamination of NB-selected samples of LAEs (which can be significant at high redshift; Hu et al. 2010; Kashikawa et al. 2011), may also strongly affect the measurements of the ACF. To test this, we assume that our mock sample of LAEs contains various fractions of low- $z$  interlopers that we model as randomly distributed sources on the sky. We see that the clustering signal is considerably decreased as the contamination fraction becomes larger (blue, green and red curves in the left panel of Figure 3). We find that the *clustering boost* due to reionization imprints the same signature as the effect of contamination on the ACF (at least at scales larger than 0.5 arcminutes). This highlights the importance of measuring ACFs over clean, i.e. spectroscopically confirmed, LAE samples in order to use the ACF as a probe of  $x_{\text{HI}}$ .

The right panel of Figure 3 shows the ACFs measured from 500 hundreds different lightcones mimicking LAE surveys at  $z = 6.6$ . We find that there is a strong variance from one realization to another and that the dispersion is of the same order as the error bars of the ACF derived by Ouchi et al. (2010) (black dots). In addition, we note that our simulated box (from which the mock lightcones are generated) is  $100h^{-1}$  cMpc on a side so we miss the density fluctuations on the largest scales. Then, on Figure 3, the level of dispersion is underestimated and must be seen as a lower limit. In addition to contamination, we also conclude that cosmic variance is certainly going to affect the detection of the *clustering boost* in LAEs surveys, and that large volumes must be probed in order to derive reliable constraints on  $x_{\text{HI}}$  using the ACF of LAEs.

## 5 Conclusions

The evolution of the statistical properties of Ly $\alpha$  emitters at  $z \gtrsim 6$  is often used as an indirect observational probe of the evolving neutral fraction of the IGM. Using a semi-analytic model of galaxy formation and numerical simulations of Ly $\alpha$  radiative transfer, we discussed the expected evolution of LAEs, ignoring the effect of reionization on their observability. Although the *intrinsic evolution* scenario as predicted by our model cannot explain quantitatively all the observations, we find that it is, at least in some cases, able to reproduce the general trends that are observed. Our results suggest that the internal evolution of galaxy properties, the LAE selection method, the contamination of photometric samples and uncertainties due to cosmic variance can sometimes account for the apparent evolution of the LAE population seen at  $z \gtrsim 6$ , and may be confused with the signature of a change in the ionization state of the IGM.

**References**

- Becker, G. D., Bolton, J. S., & Lidz, A. 2015, *PASA*, 32, e045
- Cassata, P., Le Fèvre, O., Garilli, B., et al. 2011, *A&A*, 525, A143
- Garel, T., Blaizot, J., Guiderdoni, B., et al. 2015, *MNRAS*, 450, 1279
- Garel, T., Blaizot, J., Guiderdoni, B., et al. 2012, *MNRAS*, 422, 310
- Garel, T., Guiderdoni, B., & Blaizot, J. 2016, *MNRAS*, 455, 3436
- Hatton, S., Devriendt, J. E. G., Ninin, S., et al. 2003, *MNRAS*, 343, 75
- Hu, E. M., Cowie, L. L., Barger, A. J., et al. 2010, *ApJ*, 725, 394
- Kashikawa, N., Shimasaku, K., Matsuda, Y., et al. 2011, *ApJ*, 734, 119
- McQuinn, M., Hernquist, L., Zaldarriaga, M., & Dutta, S. 2007, *MNRAS*, 381, 75
- Ouchi, M., Shimasaku, K., Akiyama, M., et al. 2008, *ApJS*, 176, 301
- Ouchi, M., Shimasaku, K., Furusawa, H., et al. 2010, *ApJ*, 723, 869
- Planck Collaboration, Adam, R., Aghanim, N., et al. 2016, *ArXiv e-prints*
- Schaerer, D., Hayes, M., Verhamme, A., & Teyssier, R. 2011, *A&A*, 531, A12
- Schenker, M. A., Ellis, R. S., Konidaris, N. P., & Stark, D. P. 2014, *ApJ*, 795, 20
- Stark, D. P., Ellis, R. S., & Ouchi, M. 2011, *ApJ*, 728, L2
- Steidel, C. C., Erb, D. K., Shapley, A. E., et al. 2010, *ApJ*, 717, 289
- Verhamme, A., Schaerer, D., Atek, H., & Tapken, C. 2008, *A&A*, 491, 89